United International Journal of Engineering and Sciences
(UIJES – A Peer-Reviewed Journal); ISSN:2582-5887 | Impact Factor:8.075(SJIF)
Volume 5 | Special Issue 1 | 2025 Edition
National Level Conference on "Advanced Trends in Engineering Science & Technology" – Organized by RKCE

Simulation Comparisons and Implementation of Induction Generator Wind Power Systems

Shaik Salam[1], Joga Pawan Kumar[2],Shaik Yasin[3] P.V. Pattabhi Ram[4]

[1,2,3,]UG Scholars, Department of Electrical and Electronics Engineering.
[4]Professor, Department of Electrical and Electronics Engineering.
[1,2,3,4,] RK College of Engineering, Vijayawada, India.

[1]Salamsathar8@gmail.com

Abstract—This paper describes the performance comparison of a wind power systems based on two different induction generators as well as the experimental demonstration of a wind turbine simulator for the maximum power extraction. The two induction machines studied for the comparison are the squirrel-cage induction generator (SCIG) and the doubly fed induction generator (DFIG). The techniques of direct grid integration, independent power control, and the droop phenomenon of distribution line are studied and compared between the SCIG and DFIG systems. Both systems are modeled in Matlab/Simulink environment, and the operation is tested for the wind turbine maximum power extraction algorithm results. Based on the simulated wind turbine parameters, a commercial induction motor drive was programmed to emulate the wind turbine and is coupled to the experimental generator systems. The turbine experimental results matched well with the theoretical turbine operation.

Index Terms—Doubly fed induction machines, field-oriented control, maximum power tracking, wind power system

I. INTRODUCTION

The increasing emphasis on renewable wind energy has given rise to augmented attention on more reliable and advantageous electrical generator systems. Induction generator systems have been widely used and studied in wind power system because of their advantages over synchronous genera tors, such as smaller size, lower cost, and lower requirement of maintenance [1], [2]. The straightforward power conversion technique using squirrel-cage induction generator (SCIG) is widely accepted in fixed-speed applications with less emphasis on the high efficiency and control of power flow. However, such direct connection with grid would allow the speed to vary in a very narrow range and thus limit the wind turbine utilization and power output. Another major problem with SCIG power system is the source of reactive power; that is, an external reactive power compensator is required to hold the distribution line voltage and prevent the whole system from overload. Onthe other hand, the doubly fed induction generator (DFIG) with variable-speed ability has higher energy capture efficiency and improved power quality and thus has attracted more attentions. With the advent of power electronic techniques, a back-to-back converter, which consists of two bidirectional converters and a dc link, acts as an optimal operation tracking interface between generator and grid [3]–[5]. Field-oriented control (FOC) is applied to both rotor- and stator-side converters to achieve desirable control on voltage and power [6], [7]. Generally, the FOC has been presented based on DFIG mathematical equations only. However, a three-phase choke is commonly used to couple the stator-side converter into the grid. Therefore, this paper proposes the FOC schemes of stator-side converter

involving the choke, and it turns out that both stator- and rotor side converter voltages consist of a current regulation part and a cross-coupling part.

First, this paper presents an experimental setup to emulate the wind turbine operation in torque control mode and thus to obtain a power operation curve for optimal power control. Second, the modeling and simulation of SCIG and DFIG wind systems are studied. Comparison between SCIG without static var compensator (STATCOM) and SCIG with STATCOM as well as DFIG system clearly indicates difference in resulted distribution line voltage.

The paper is organized as follows. The wind turbine is modeled and simulated using the turbine emulator, and an ex pression of optimal output power versus rotor speed is proposed in Section II. In Section III, the SCIG wind power system is es tablished based on wind turbine system described in Section II. In addition, the DFIG is introduced by mathematical model in Section IV, indicating the relationship of voltage, flux, and torque. At last, steady-state and dynamic experiment/simulation results are presented and discussed in Section V

II. WIND TURBINE

Wind energy is extracted through wind turbine blades and then transferred by the gearbox and rotor hub to the mechanical energy in the shaft, which drives the generator to convert the mechanical energy to electrical energy**.**

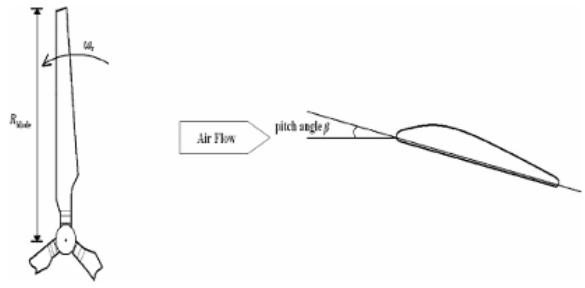

Fig. 1. Schematics of turbine blade from different views.

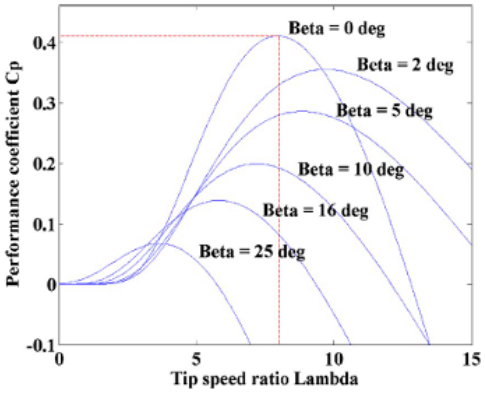

Fig. 2. $C_p-\lambda$ curve for the turbine model.

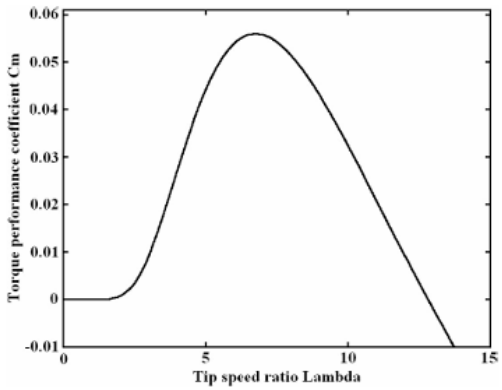

Fig. 3. $C_m-\lambda$ curve for the turbine emulator.

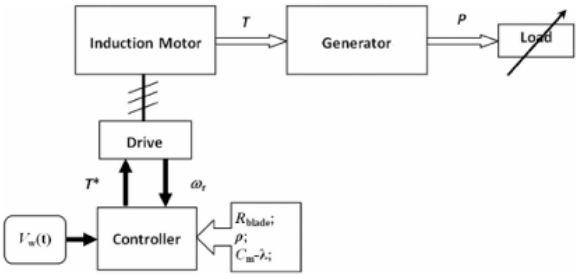

Fig. 4. Wind turbine emulator system.

where Pm is the mechanical output power in watts, which depends on power performance coefficient Cp, air density ρ, turbine swept area A, and wind speed vw. (1/2) · ρAv3 w is equalto the kinetic energy contained in the wind at a particular speed vw. The performance coefficient Cp(λ,β), which depends on tip speed ratio λ and blade pitch angle β, determines how much of the wind kinetic energy can be captured by the wind turbine system. A nonlinear model describes Cp(λ,β) as [8]. the blade radius and angular frequency of rotational turbine as depicted in Fig. 1. The Cp−λ curve for this particular turbine model at different β is shown in Fig. 2 where it is illustrated that, to achieve maximum Cp, one has β =0◦ and λ =8. The blade with fixed geometry will have fixed Cp−λ characteristics, as described in (2) and (3). Therefore, to track the optimal output power, the curve of Pm−ωr is the "map" to follow.Thus, based on turbine Cp−λ model andby assuming β =0◦, theCm−λ curve is given in Fig. 3. At any particular vw, one could obtain different torque and, thus, power output by varying rotor speed. The system configuration is shown in Fig. 4, where the ωr is fed back to the controller for calculating Cm and, then, torque command.

III. SCIG WIND POWER SYSTEM

Fig. 5 shows the schematics of the SCIG system including the wind turbine, pitch control, and reactive power compensator. The entire system includes three stages for delivering the en ergy from wind turbine to the power grid. The first one is wind farm stage which handles with low voltage Vwt, the second is distribution stage which has medium voltage Vdis, and the third is grid transmission stage which has high voltage Vgrid. The three-phase transformers take care of the interface between stages [9]. As mentioned, nominal power PnSCIG is considered as active power reference to regulate the pitch angle while Vdis and Idis denote the distribution line-to-line voltage and phase current, and they are monitored to favor the reactive power compensation for distribution line. This fairly straightforward technique was first used since it is simple and has rugged construction, reliable operation, and low cost. However, the fixed-speed essential and potential voltage instability problems severely limit the operations of wind turbine [1], [3]. Since SCIG is of fixed-speed generator, for a particular wind speed, the output active power is fixed as well. Thus, with the increase of wind speed, so does the output power until the nominal power is reached. The wind speed at this moment is called nominal wind speed. Beyond this speed, the pitch angle system will prevent the output power from exceeding the nominal value.

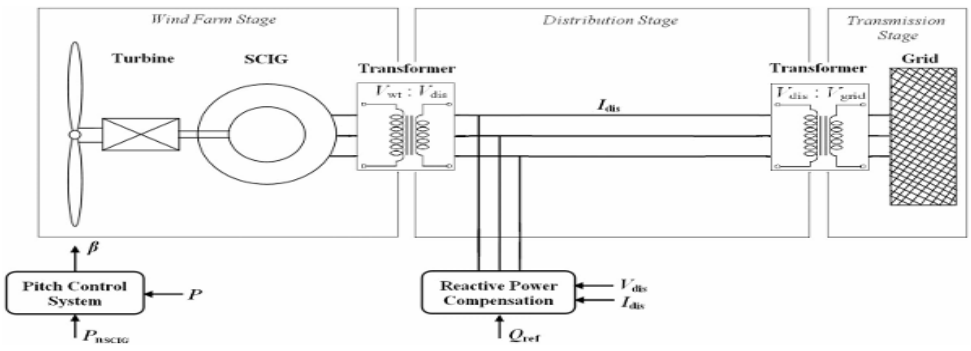

Fig. 5. SCIG wind power system topology.

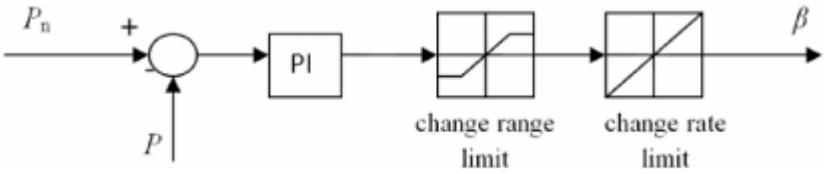

Fig. 6. Pitch angle control.

That is, when the wind speed is below nominal value, the power capture can vary with the change of wind speed; and when the wind speed is above nominal value, the pitch angle control system will limit the generated power by changing the pitch angle. In such way, the output power will be stabilized at nominal value where the wind speed is always above nominal speed. Thepitch angle is determined by an open loop control of regulated output active power and by that shown in Fig. 6. Due to the huge size of blade and, thus, inertia, pitch angle has to change in a slow rate and a reasonable range. It is also worthy to notice that, without reactive power source, in Section V, the SCIG system tends to lead to a voltage droop in distribution line which will cause overload problem. In the simulation section, the comparison between SCIG system with and without STATCOM is conducted.

IV. DFIG WINDPOWER SYSTEM

Traditionally, the dynamic slip control is employed to fulfill the variable-speed operation in wind turbine system, in which the rotor windings are connected to variable resistor and con trol the slip by the varied resistance [3], [10]. This type of system can achieve limited variations of generator speed, but external reactive power source is still necessary. Consequently, to completely remove the reactive power compensation and to control both active and reactive power independently, DFIG wind power system is one of most popular methods in wind energy applications [1], [3], [7]. This paper reproduces DFIG model first of all and then concentrates on the controlling schemes of power converters, in which the active and reactive power are controlled independently. In particular, the stator-side converter control involving an RL series choke is proposed.

Both controlling of rotor- and stator-side converter voltages end up with a current regulation part and a cross-coupling part. The wind turbine driving DFIG wind power system consists of a wound-rotor induction generator and an ac/dc/ac insulated gate bipolar transistor (IGBT)-based pulse width-modulated (PWM) converter (back-to-back converter with capacitor dc link), as shown in Fig. 7. In this configuration, the back-to-back converter consists of two parts: the stator-/grid-side converter and the rotor-side converter. Both are voltage source converters using IGBTs, while a capacitor between two converters acts as a dc voltage source. The generator stator windings are connected directly to grid (with fixed voltage and frequency of grid) while the rotor winding is fed by rotor-side converter through slip rings and brushes, at variable frequency.

United International Journal of Engineering and Sciences
(UIJES – A Peer-Reviewed Journal); ISSN:2582-5887 | Impact Factor:8.075(SJIF)
Volume 5 | Special Issue 1 | 2025 Edition
National Level Conference on "Advanced Trends in Engineering Science & Technology" – Organized by RKCE

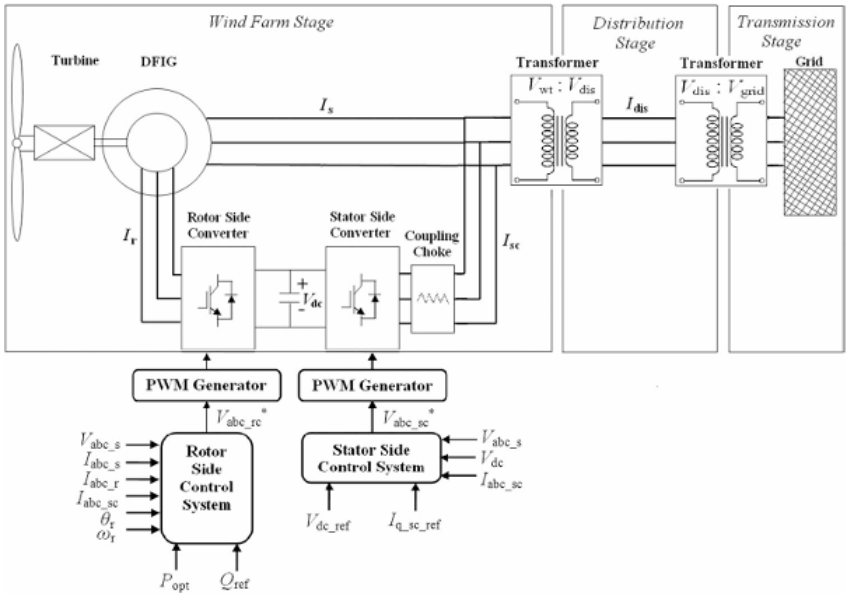

Fig. 7. Wind turbine–doubly fed induction generator system configuration.

A. **Rotor-Side Converter Control**

Because of being directly connected to the grid, the stator voltage shares constant magnitude and frequency of the grid. One could make the d-axis align with stator voltage vector; it is true that Vs = Vds and Vqs =0, thus Ψs =Ψqs and Ψds =0, which is of stator-voltage-oriented vector control scheme, asdepicted in Fig. 9. According to (7)–(9), the rotor-side converter reference current.

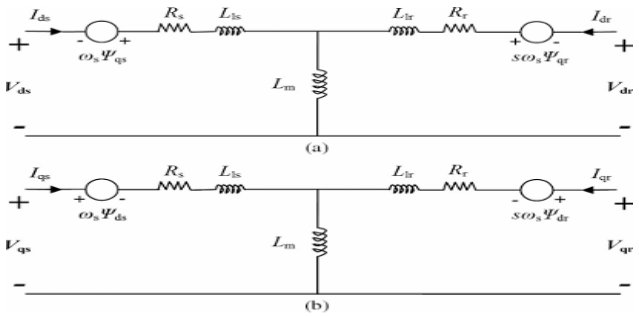

ig. 8. Equivalent circuit of DFIG. (a) *d*-axis model. (b) *q*-axis model.

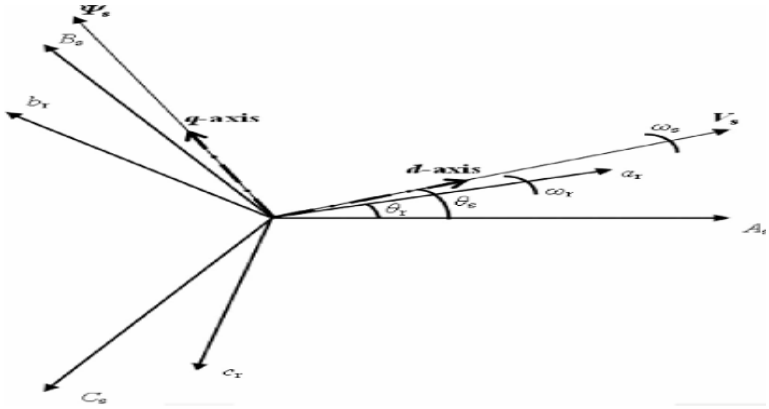

Fig. 9. Stator voltage FOC reference frame.

Ploss are desired optimal output active power, reference active power, and system power loss. Combining (10)–(12), the active power is used as command inputs to determine current refer ence Idr_ref. Meanwhile, the output reactive power is the stator reactive output power since the stator-side converter's reactive power is set to be zero.

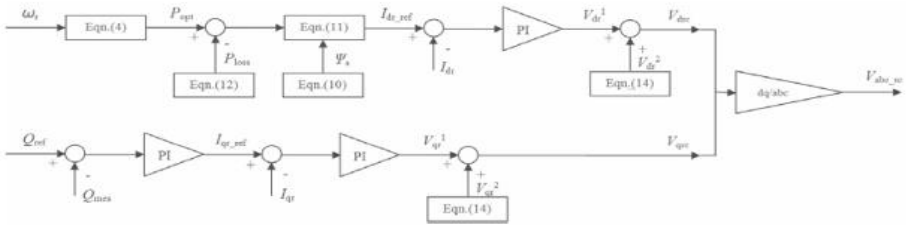

Fig. 10. Rotor-side converter control scheme.

B. Stator-Side Converter Control

Concerning the use of three-phase series RL choke between stator- and stator-side converter, a cross-coupling model is required to derive the voltage signal of stator-side converter, as described in Fig. 11Moreover, V 1 dch and V 1 qch are determined by the regulation of currents Idsc and Iqsc in which the current reference Iqsc_ref is given directly while Idsc_ref is determined by the regulation of dc-link voltage Vdc. Thus, above all, the stator-side converter voltage signals Vdsc and Vqsc are obtained as follows and depicted in Fig. 12

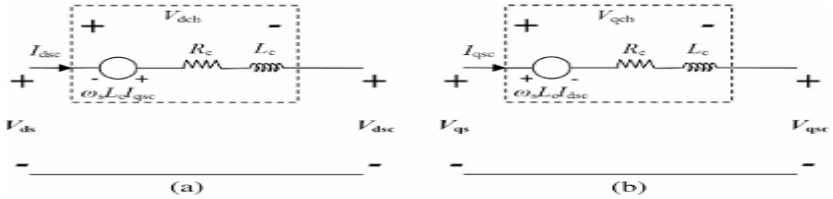

Fig. 11. Equivalent circuit of stator-side-converter choke. (a) d-axis model (b) q-axis model.

V. EXPERIMENTAL AND SIMULATION RESULTS

A. Wind Turbine and Operation Curves

The experimental wind turbine emulator system is shown in Fig. 13, where a 3-hp induction motor, driven by ABB ASC550 was operated in torque-control mode to simulate a turbine. The wind turbine model is programmed into the DSP based control card from microchip. The controller takes the windturbine parameters and operating conditions from the user. Moreover, the controller measures the generator speed and then produces the torque command to the induction machine drive. A generator system is coupled to the induction motor to be able to apply variable loading conditions.

For a given wind speed of vw =13m/s, the T−ωr char acteristics are simulated by implementing different operation points on the curve. By varying generator load, the rotor speed and Cm are varied according to (1)–(4), and the torque is calculated in DSP and fed to generator. It is shown in Fig. 14 that the operation points of the experimental system match those derived from theoretical calculations. These experimental

of Fig. 14. The torque and speed quantities are presented in per unit (p.u.) as base turbine torque being 41 N · m and base turbine speed being 553.8 r/min, which leads to 0.457-p.u. torque and 0.7-p.u. speed for point A. Similarly, the torque and speed are 0.96 and 1.157 p.u., respectively, for point B. The experimental power results are scaled into p.u. by base power of 1116.8 W.Theresults are plotted in Fig. 17, indicating an optimal power operation point at C, where the power is maximum for this particular wind speed. The other optimal power operation points for different wind speeds are emulated in the same way so that the optimal power curve can be applied as a reference to the generator controller. In this paper, for different wind speeds and fixed β =0◦, the Pm−ωr curve is presented in Fig. 18 for wind speeds ranging from 6 to 14 m/s. By connecting the maximum points of all curves, the relationship between maximum output power and the rotor speed

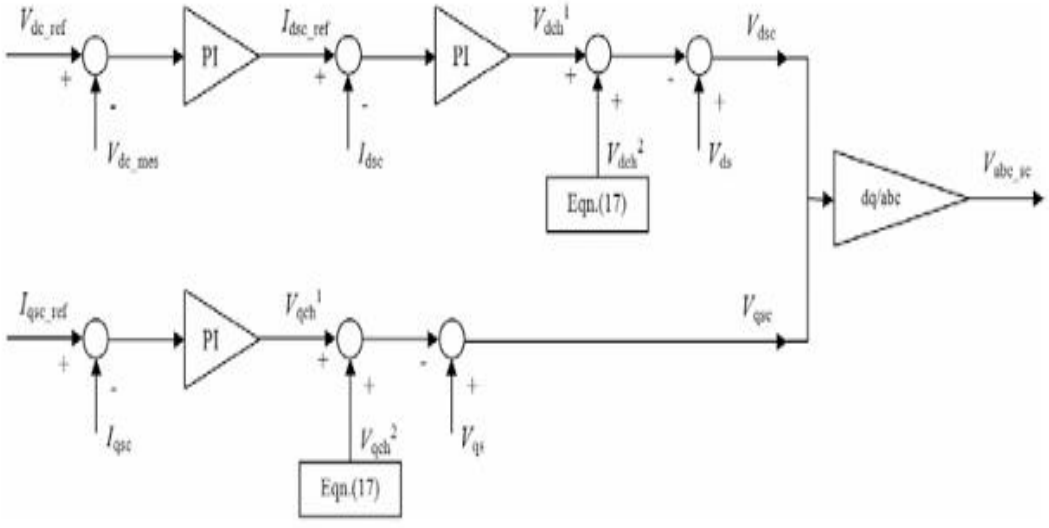

Fig. 12. Stator-side converter control scheme.

Fig. 12. Stator-side converter control scheme.

Fig. 13. Experimental setup for wind turbine emulator.

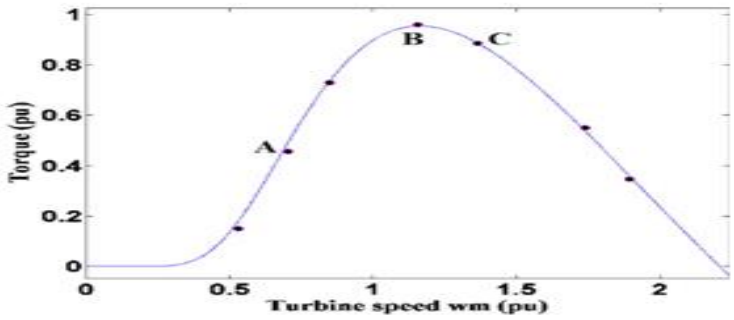

Fig. 14. Experimental turbine operation torque results (solid line refers to theoretical result; spots refer to experimental results).

TABLE I
WIND TURBINE EXPERIMENTAL SYSTEM PARAMETERS (v_w = 13 m/s)

ω_m (pu)	T (pu)	I_a (A)	R_{load} (Ω)	P_{load} (W)
0.531	0.15	2	8	32
0.704	0.457	14	1.2	235.2
0.849	0.729	23	1	529
1.156	0.96	32	1	1024
1.366	0.885	29.8	1.3	1154.5
1.74	0.55	17	3.2	924.8
1.895	0.347	8.7	7	529.8

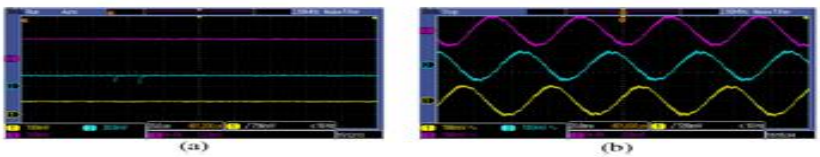

Fig. 15. Operation point A of Fig. 14. (a) (Lower trace) Torque. (Middle trace) Speed. (Upper trace) Armature current using 1/50 probe. (b) Phase currents of induction motor—10 mV/A.

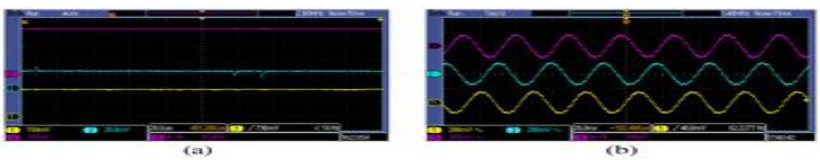

Fig. 16. Operating point B on Fig. 4 (a) (1) Torque. (2) Speed. (3) Armature current—1/50 probe. (b) Phase currents of induction motor—10 mV/A).

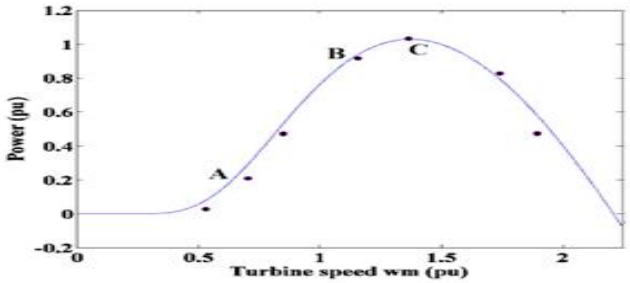

Fig. 17. Experimental turbine operation power results (solid line refers to theoretical result; spots refer to experimental results).

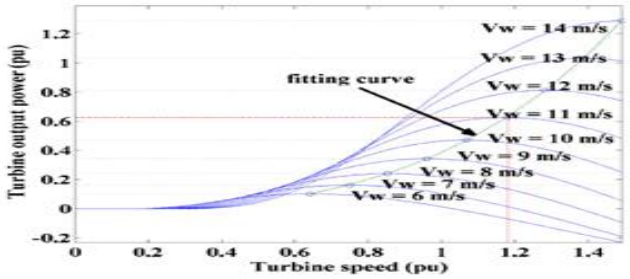

Fig. 18. $P_m - \omega_r$ curve for the turbine model.

TABLE II
SCIG-BASED WIND POWER SYSTEM PARAMETERS

Parameter	Value
Nominal Wind Speed v_w	11 m/s
Nominal Active Power P_{nSCIG}	0.855 MW
Grid Voltage V_{grid}	120 kV
Grid Frequency f_{grid}	60 Hz
Distribution Line Voltage V_{dis}	12.5 kV
Wind Turbine Bus Voltage V_{wt}	575 V
Stator Resistance R_s	0.0048 p.u.
Stator Leakage Inductance L_s	0.1248 p.u.
Rotor Resistance R_r	0.0044 p.u.
Rotor Leakage Inductance L_r	0.1791 p.u.
Mutual Inductance L_m	6.77 p.u.
STACOM Constant Voltage V_{dc}	4 kV
STACOM Equivalent Capacitance C	625 μF

B. SCIG

A traditional SCIG wind power system is developed in Matlab/Simulink, and the related system data used are given in Table II. In order to investigate the system performances, a ramp wind speed vw is assumed that varies from t =10stot =16s and, then, it remains constant to the end of simulation t =40s. Fig. 19(a)–(e) shows the dynamic variations and steady states of pitch angle β, generator speed ωr, produced active power P, and consumed reactive power Q. First, the fluctuation in theresults during t =0 to 2.5 s is due to the initial conditions. In the simulation, the initial speed of generator is set at slip s =−0.01p.u. with respect to synchronous speed and, then, re sponse to the wind speed input disturbance. Other initial values for power and voltages are zero. The steady-state results for vw =8m/s indicate the operation points ωr =1.0015p.u. and P =0.29MWonFig.18. Since it is lower than nominal value of 0.855 MW,pitchanglecontrol is not working. After t =10s, with the increase of vw,sodotheωr and P until t =13s when vw exceeds the nominal value (11 m/s). This is because the pitch control is triggered to limit the increase of output power P and Q as shown in Fig. 19(b)–(d). In this way, the pitch control effectively limits the output P around the nominal value of 0.855 MW and settles a new pitch angle at roughly t =17s. This nominal operation point can also be observed in Fig. 18 (vw =11m/s;P =0.855 MW;ωr =1.005 p.u).

It is noted that the rotor speed can only vary in very small scope around 1 p.u. (fixed-speed system) and, thus, impossible to achieve optimal active power output. Thus, the active power outputs at vw =8m/s and ≥ 11 m/s in SCIG are 0.29 and 0.855 MW which are lower than those in later DFIG system. Also, without independent control ability, SCIG system con sumes reactive power of 0.41 Mvar in the steady state, which will lead to line voltage droop. To provide necessary reactive power, a STATCOM is added on the distribution line to inves tigate the improvement. As in Fig. 20, distribution line voltage can drop by approximately 0.055 p.u. in SCIG system without STATCOM, which will be a potential induction of overload in system. In contrast, SCIG system with STATCOM can hold distribution voltage to 0.99 p.u. and favorable to grid system stability. The compensated reactive power from STATCOM is shown in Fig. 21 and is equal to 0.3 Mvar in the steady state, a little bit less than the real consumed value in Fig. 19(d). Although STATCOM provides impressive help on constant distribution line voltage, the DFIG presents better result and does not need the help from STATCOM, as shown in Fig. 20 .

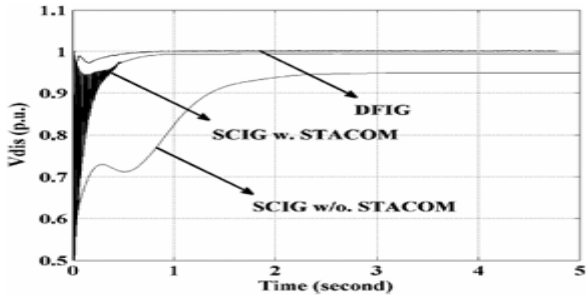

Fig. 20. Distribution voltages for SCIG system with/without STATCOM a DFIG system.

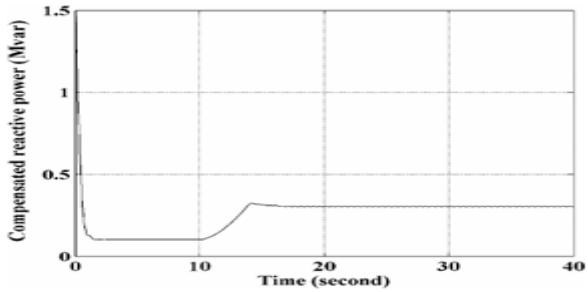

Fig. 21. STATCOM compensated reactive power.

C. DFIG

By using the proposed optimal power curve as well as the system parameters listed in Table III, the DFIG wind power system is simulated. The DFIG system allows the optimal (maximum) output power operation in the absence of reactive power source. Also, the independent control of active and reactive power is achieved. In the Matlab/Simulink model, the converter switch fre quency is set to be 27 times the grid frequency f. To achieve acceptable accuracy, the power circuit and the control circuit models are discretized at different time steps. It is worthy to note that the nominal apparent power and nominal active power are considered as nominal electrical power and nominal me chanical power in this wind power system [3], [13]. Simulation and control system parameters are listed in Table IV and are preloaded into workspace before running the simulation and easy to be

modified in m file. First of all, the steady-state results of the system are shown in Fig. 22(a)–(d), where four wind speed cases vw = 7, 9,10, and 12 m/s to verify the optimal power output tracking are presented. All of them kept the bus voltage at 1200 Vdc, indicating the well operation of stator-side converter, while the reactive power is set to be zero as the input command. In order to track the optimal active power output, optimal rotor speeds are implemented accordingly. For instance, one could recall inFig. 18 that, at vw =7m/s, the optimal output active power is 0.17 p.u. with nominal power of 1.5 MW, i.e., 0.255 MW. A little bit power droop could be observed from simulation results which are caused by power loss in (12). Meanwhile, the optimal rotor speed is also achieved at 0.75 p.u., same as the value in Fig. 18. Similarly, the optimal trackings of output power and rotor speed are exhibited in other wind speed cases as well. Therefore, it can be concluded that the system works well to follow the optimal power control at steady-state operation. It is noticed that P and Q are vanished during the first cycle (1/60 s) in displayed result because of the calculation time cost.

TABLE III
DFIG-BASED WIND POWER SYSTEM PARAMETERS

Parameter	Value
Nominal Wind Speed v_w	11 m/s
Nominal Apparent Power S_e	1.67 MVA
Nominal Active Power P_{nDFIG}	1.5 MW
Power Factor pf	0.9
Grid Voltage V_{grid}	120 kV
Grid Frequency f	60 Hz
Distribution Line Voltage V_{dis}	12.5 kV
Wind Turbine Bus Voltage V_{wt}	575 V
Generator Number of Pole Pairs n_p	3
Stator Resistance R_s	0.0071 p.u.
Stator Leakage Inductance L_s	0.171 p.u.
Referred Rotor Resistance R_r	0.005 p.u.
Referred Rotor Leakage Inductance L_r	0.156 p.u.
Stator-to-Grid Coupling Resistance R_c	0.003 p.u.
Stator-to-Grid Coupling Inductance L_c	0.3 p.u.
Mutual Inductance L_m	2.9 p.u.
Nominal DC-link Voltage V_{dc}	1.2 kV
DC-link Capacitance C	10 mF
Maximum C Converter Current I_{conv_max}	0.5 p.u.
System Inertia Coefficient H	5 second
Generator Friction Damping F	0.01 p.u.

TABLE IV
SIMULATION AND CONTROL PARAMETERS

Parameter	Value
Power System Sampling Period T_{s_Power}	5e-6 sec
Control System Sampling Period $T_{s\_Control}$	1e-4 sec
Switch Frequency f_{sw}	1620 Hz
Transmission Distance D_{tran}	30 km
Reactive Power Regulator Coefficients K_p; K_i	0.05; 5
DC-link Voltage Regulator Coefficients K_p; K_i	0.002; 0.1
Rotor-side Current Regulator Coefficients K_p; K_i	0.3; 8
Stator-side Current Regulator Coefficients K_p; K_i	2.5; 500

Second, the system dynamic response to varied wind speeds is investigated. Due to the large H of the system, dynamic vari ation can last and be observed in a long time period before con verging to the steady-state values. To shorten such period, H = 0.1 s is used in this part of simulation. With stable steady-state initial values, three regular types of wind speeds are examined for dynamic responses, including step, ramp, and gusty winds. The varied winds and corresponding results for Vdc, ωr, P, and Qare shown in Figs. 23 and 24, where the system can always reach a new optimal steady state after a few seconds. In the aforementioned results, the reduced inertia constants can only

decrease the converging time, making the system reach a new steady state quicker, and it has no effects on steady-state values. At last, the system dynamic response to a grid disturbance is investigated. At vw =9m/s, a remote voltage droop in grid is programmed from t =0.09 to 0.29 s. The dynamic responsesare presented in Fig. 24. During this process, since the wind speed remains the same, control system effectively makes the system recovers in approximate 0.1 s.

D. Comparison Between Two Systems

A summary of SCIG and DFIG systems is presented in Table V based on research of this paper. The comparison shows the superiority of DFIG system over SCIG system in terms of efficiency, controllability, and high-power applications. Also,the higher cost of slip rings and power electronics can be compensated by more power output.

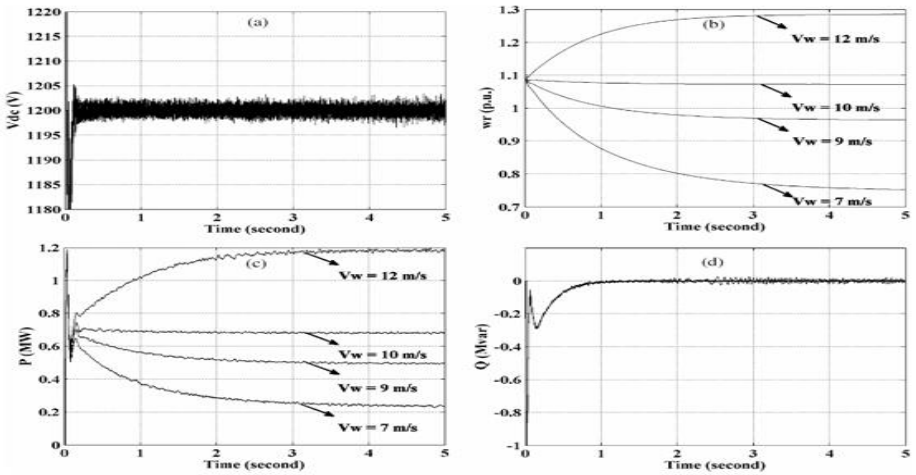

Fig. 22. System responses to different constant wind speeds. (a) DC-link voltage V_{dc}. (b) Rotor speed ω_r. (c) Active power P. (d) Reactive power Q.

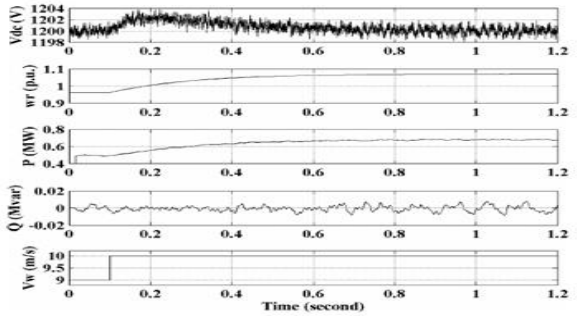

Fig. 23. Wind step response. (a) DC-link voltage V_{dc}. (b) Rotor speed ω_r. (c) Active power P. (d) Reactive power Q. (e) Wind speed v_w.

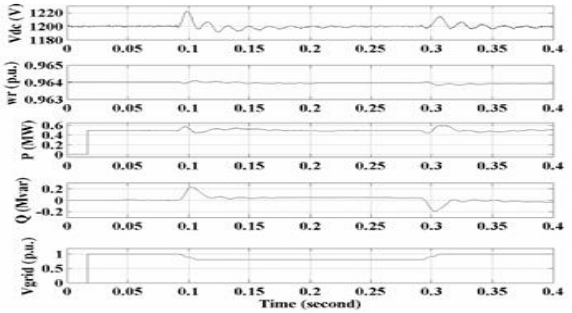

Fig. 24. Dynamic responses to grid voltage droop. (a) DC-link voltage V_{dc}. (b) Rotor speed ω_r. (c) Active power P. (d) Reactive power Q. (e) Grid voltage V_{grid}.

VI. CONCLUSION

This paper has presented the comparison of the wind turbine systems using SCIG and DFIG generator systems. With the experimentally investigated wind turbine model, a SCIG and a DFIG wind power systems are modeled and simulated inMatlab/Simulink. An optimal active-power-versus-rotor-speed relationship has been proposed for turbine model first, and it functions as a lookup table for tracking the maximum output active power. The SCIG system presents the need of external reactive power source to support grid voltage, and it can keep the output power at the nominal level by pitch control but cannot accordingly change the rotor speed to achieve maximum wind power capture at different wind speeds. In contrast, the DFIG system does not need reactive power compensator to hold distribution line voltage and achieves optimal active power controlling. Both voltage control schemes for two converters consist of a current regulation part and a cross-coupling part. The turbine emulator system performs well and follows the theoretical and simulated maximum power extraction points in different operating conditions.

TABLE V
SUMMARY OF SCIG AND DFIG WIND POWER SYSTEMS

	SCIG	DFIG
Speed Operation	fixed or limited variable	variable
Line Voltage	drop by 0.05 p.u.	stable constant
Control Scheme	pitch control	FOC
Active Power	varies with v_w but not optimally	varies with v_w optimally
Reactive Power	uncontrollable; need compensation	controllable
Power Rating	< 1MW	> 1MW
Cost and Complexity	low and simple	high

REFERENCES

[1] M. Orabi, T. Ahmed, and M. Nakaoka, "Efficient performances of in duction generator for wind energy utilization," in Proc. 30th Annu. Conf. IEEE Ind. Elect. Soc., Nov. 2004, pp. 838–843.

[2] M. Molinas, J. A. Suul, and T. Undeland, "Low voltage ride through of wind farms with cage generators: STATCOM versus SVC," IEEE Trans. Power Electron., vol. 23, no. 3, pp. 1104–1117, May 2008.

[2] M. Molinas, J. A. Suul, and T. Undeland, "Low voltage ride through of wind farms with cage generators: STATCOM versus SVC," IEEE Trans. Power Electron., vol. 23, no. 3, pp. 1104–1117, May 2008.

[4] Y. Lei, A. Mullane, and G. Lightbody, "Modeling of the wind turbine with a doubly fed induction generator for grid integration studies," IEEE Trans. Energy Convers., vol. 21, no. 1, pp. 257–264, Mar. 2006.

[5] R. Ganon, G. Sybille, and S. Bernard, "Modeling and real-time simula tion of a doubly-fed induction generator driven by a wind turbine," pre sented at the Int. Conf. Power Systems Transients, Montreal, QC, Canada, Jun. 2005, Paper IPST05-162.

[6] H. Sun, Y. Ren, and H. Li, "DFIG wind power generation based on back to-back PWM converter," in Proc. IEEE Int. Conf. Mechatron. Autom., Aug. 2009, pp. 2276–2280.

Yu Zou received the B.S. and M.S. degrees in elec trical engineering from Tianjin University, Tianjin, China, in 2004 and 2007, respectively, and the Ph.D. degree from the Department of Electrical and Com puter Engineering, The University of Akron, Akron, OH, USA, in 2012. He is currently an Assistant Professor with the Department of Electrical and Computer Engineering, Saginaw Valley State University, University Center, MI, USA. His research interests include power electronics and electric machine controls.

Yu Zou received the B.S. and M.S. degrees in elec trical engineering from Tianjin University, Tianjin, China, in 2004 and 2007, respectively, and the Ph.D. degree from the Department of Electrical and Com puter Engineering, The University of Akron, Akron, OH, USA, in 2012. He is currently an Assistant Professor with the Department of Electrical and Computer Engineering, Saginaw Valley State University, University Center, MI, USA. His research interests include power elec tronics and electric machine controls.

Yilmaz Sozer (M'04) received the B.S. degree in electrical engineering from the Middle East Techni cal University Ankara, Ankara, Turkey, and the M.S. and Ph.D. degrees in electric power engineering from Rensselaer Polytechnic Institute, Troy, NY, USA. His graduate work focused on power electronics and the development of control algorithms for electric machines. Before joining the faculty of the Department of Electrical and Computer Engineering, The Univer sity of Akron, Akron, OH, USA, after the comple tion of his doctorate degree, he worked with Advanced Energy Conversion, Schenectady, NY, USA. He is currently an Assistant Professor with the De partment of Electrical and Computer Engineering, The University of Akron, engaged in teaching and research. His research interests are in the areas of control and modeling of electrical drives, alternative energy systems, design of electric machines, integrated and belt-driven starter/alternator systems, high power isolated dc/dc converter systems, large industrial static power conversion systems that interface energy storage, and distributed generation sources with the electric utility. Dr. Sozer has been involved in IEEE activities which support power elec tronics, electric machines, and alternative energy systems. He is serving as an Associate Editor for the IEEE Industry Applications Society (IAS) Electric Ma chines Committee and Secretary of the IEEE IAS Sustainable and Renewable Energy Systems Committee.